Knowledgeable Research (KR)
ISSN: 2583-6633 | CODEN: KRABAU
International Open-Access Peer-Reviewed Refereed Multidisciplinary Journal
https://knowledgeableresearch.com
Vol. 5, Issue 05, May,2026

Received: 06/04/2026 | Accepted: 22/05/2026 | Published: 30/05/2026

Determination of Jones-Wilkins-Lee equation of state parameters using artificial neural network;Accuracy verification by coupled with experiment and numerical simulation

Ik Hyon Mun[1], Jin Guk Pak[2], Chol Min Kim[3], Jong Ju Kang[4], Chang Song Paek[5], Jong Hyok Kim[6]*

High-Tech Research and Development Center, **Kim Il Sung** University, Pyongyang, Democratic People's Republic of Korea.

Abstract

A method for determining the JWL parameters and the detonation parameters using artificial neural networks is presented. The JWL EOS parameters and detonation parameters were collected according to composition of explosives, density and formation heat for 91 materials. The neural network model consists of the input, layer, output layer and hidden layer, and used the Neural Network Fitting Tool of Matlab, and Levenberg-Marquardt backpropagation algorithm was used for network training.The rational neural network architecture has 237, 179 and 72 neurons in three hidden layers, respectively, and the fit is reasonably good for for training, validation, and test sets, with R values in each case of above 0.99. The JWL EOS parameters were predicted for some explosives, 95RDX/3WAX/2stearic acid, 60TNT/24RDX/16Al, and 50AP/25Al/25RDX.Using trained neural network, we evaluated the JWL state equation parameters and detonation parameters for three explosives with two densities, respectively, and coupled with numerical simulations and experiments to evaluate the generalization performance of the neural network. The relative error between the predicted detonation velocity values and detonation velocity values determined by Pin Oscillographic Technique is less than 5%.And also, the relative error between the experimental values and the explosion shock overpressure values obtained by numerical simulations using AutoDyn is less than 5%.

Keywords: *JWL equation of state parameter, artificial neural network, explosion shock wave, detonation velocity, numerical simulation*

***Corresponding Author:**
Jong Hyok Kim
Email: jh.kim1030@star-co.net.kp

1. Introduction

The calculations of explosion charateristic involve the calculation of the equilibrium composition of the detonation products at a given pressure and temperature, and the accuracy of the calculation of the detonation product composition will have a great impact on the accuracy of the explosion charateristic calculations. The calculation of the composition of the detonation products is carried out by the Gibbs free energy minimization method reasonably, but its accuracy depends largely on the accuracy of the thermodynamic state quantity of the detonation products. Therefore, to increase the accuracy of the detonation parameters calculation, it must determin correctly the

thermodynamic state quantities of the detonation products using the state equations of the detonation products corresponding to the detonation state of the explosives. Also, In order to calculate the explosion characteristics accurately and to accurately simulate the target failure process by the detonation of the explosive and the expansion of the detonation product, the state equation of the detonation product must be given.

Thus, in the evaluation of the destructive action effectiveness of explosives and the study and calculation of the explosive composition design, the choice of the state equation of detonation products is very important and many detonation product state equations have been proposed up to now.

First, there is a purely theoretical form of determination, starting from certain assumptions, such as the multi-exponential state equations and VLM state equations, independent of the explosive explosion test data. The several empirical or semi-empirical detonation product state equations have been proposed, such as BKW (Becker-Kistiakowsky-Wilson), KHT (Kihara-Hikita-Tanaka), VLW, LJD (Lennard-Jones-Devonshire), JWL Jones-Wilkins-Lee, these state equations are state equations which considered chemical reaction, except the JWL state equation among above mentioned state equations.[1-3]

In order to use the state equations above mentioned, the composition of the detonation products must be known, corresponding to each moment of expansion of the detonation products, so there are limitations in use by the complexity of the calculations and the high computational cost. As the state equation without considering chemical reaction, the empirical JWL state equation of detonation products is the most widely used state equation among the state equations known so far. The Jones-Wilkins-Lee state equation is a widely used state equation for explosion simulation in custom applications such as ANSYS AUTODYN and LS-DYNA, not only because it accurately reflects the expansion process of the detonation products, but also because it is convenient to use in comparison with other state equations.

The JWL state equation is the state equation describing the relationship between the pressure, specific volume and internal energy of the detonation product, which is given by

$$p(\bar{v},E)=A\left(1-\frac{\omega}{R_1\bar{v}}\right)e^{-R_1\bar{v}}+B\left(1-\frac{\omega}{R_2\bar{v}}\right)e^{-R_2\bar{v}}+\frac{\omega E_0}{\bar{v}} \quad (1)$$

Here

p —The pressure of the detonation products, GPa

$\bar{v}$ —Relative volume of detonation products, cm^3/g

$$\bar{v}=\frac{v}{v_0}=\frac{\rho_0}{\rho} \quad (2)$$

v_0 , v —Initial specific volume of explosive and specific volume of detonation products, cm^3/g

A, B, R_1, R_2, ω—Constants related to explosives

E —Internal energy per unit volume of detonation products, GPa

A typical experimental method for determining the parameters of the JWL state

equation is the cylinder expansion test. The cylinder expansion test (CYLEX) test) using oxygen-free high conductivity (OFHC) copper cylinder with very good ductility which is not broken even when expanded to two to three times the initial radius, is a standardized experiment specifically used to determine the parameters of the JWL state equation and to evaluate the working capacity of explosives [4, 5]. The process of explosion expansion of a copper cylinder filled with explosives in air is evaluated in relation to the cylinder wall expansion displacement, velocity and time using optical instruments or ionization pins [6, 7], equipped with a set of gold-plated probes and a high-speed pulse timer [8, 9]. The strong correlation between the underwater shock wave and the expansion wave produced by the expansion of detonation products was confirmed in underwater explosion test. So it can estimate the relation between the pressure and volume in the expanded region of detonation products, finally can detemine the parameters of JWL EOS. As mentioned above, the experimental methods for determination of JWL EOS requires expensive equipment and complicated auxiliary equipment, long time and effort. The main methods for evaluating the characteristics of explosives without experiment in the field of explosive research include empirical, thermochemical, quantum chemical and machine learning methods. The most typical example of an empirical method is the Kamlet Jacobs formula, which can be used to simply obtain the detonation parameters, given composition of the explosive. However, although these empirical methods are convenient and simple to use, their application range is limited, especially for new explosive compositions or molecules, which are difficult to ensure accuracy. Theoretical methods have been proposed to determine the JWL state equations using various thermochemical calculation method, e.g., Becker-Kistiakowsky-Wilson (BKW), Kihara-Hikita-Tanaka (KHT), but these methods have some limitations. In other words, the BKW or KHT equations of state are state equations that well reflect the detonation state of the explosive, but the JWL equation of state is a EOS that reflect the explosion expansion whole process, so the theoretical method based on the BKW or KHT equation of state for determination the JWL EOS parameters, which is relatively accurate near the detonation state but with large errors in the explosion expansion stage.

Thus, thermochemical calculations based on various state equations can be applied to new explosives or composite explosives composed of different components, but this method cannot completely reduce the error [10]. Also, a large computational time and computational effort are needed to involve complex product composition calculations to apply the state equation to the analysis of the explosion process. Quantum chemical methods such as density functional theory are applicable to different objects, but it requires long computational time, and also it is difficult to obtain accurate results without significant computational resources [11].

In recent years, ANN-based machine learning methods have been gradually applied to character prediction of explosives [12, 13]. The machine learning approach can produce reasonable prediction results after training using a training set and has advantages such as simple use, fast prediction, and satisfaction with engineering requirements. The algorithm between the initial parameters of the explosive, such as composition and loading density, and the parameters of the JWL EOS is difficult. Therefore, applying a machine

learning method with superior adaptability, called learning and self-organization, can predict the JWL EOS parameters quickly by teaching a large number of information of the experimentally determined JWL EOS parameters according to initial parameters in the neural network.

The aiticle for the determination of the JWL equation of state parameters is organized as follows.

In section2, a training set was constructed by collecting the JWL state equation parameters for single and composite explosives, and a reasonable neural network model was introduced. And the results after model training are discussed.

In section3, the JWL state equations of the new composite explosives were determined using constructed rational the neural network model.

Then, verified the generalization performance of the neural network model by coupled with numerical solution and experiments. Section4 presents the conclusions.

2. A neural network model for JWL EOS parameters prediction

2.1. Database construction

Explosive can be divided into single and mixed explosives according to composition. Single explosives include TNT, RDX, HMX, PETN, Tetryl, HNS, CL-20, and composite explosives are composed of single explosives and other additives (such as paraffins, binders such as ESTANE, oxidants such as AP, and metal powders such as Al). The composition of a single explosive or aluminized explosive can be calculated as the number of individual elements and the composition of different explosives can be expressed by general formula ($C_aH_bO_cN_dAl_eCl_fF_g$). Therefore, the initial parameters of the explosive must reflect the number of elements C, H, N, O, Al, Cl and F. However, even though the same general formula is used, different compositions of explosive may lead to different explosion properties, so the formation enthalpy of explosives should be the initial parameter of explosives so that the influence of the composition can be considered. Also, an important point to consider is that in practice, for an explosive of the same composition, the loading density should be set as one of the initial conditions, since the explosion process of explosive charge will also be different if the loading density is different. Hence, number of elements, formation enthalpy and loading density were set as input data, and also the parameters of JWL EOS, detonation velocity and detonation pressure were set as the output data. The number of elements and formation enthalpy are calculated for 1 kg of explosive, respectively. The parameters of the JWL EOS, detonation velocity and detonation pressure data according to the number of elements, loading density and formation enthalpy used as training data for neural networks are given in Table 1.

2.2 Neural network model establishment

Estimation problem for parameters of the JWL EOS is a neural fitting problem between a data set of numeric inputs and a set of numeric targets. Therefore, all calculations are performed using the Neural Network Fitting Tool of Matlab, and the neural network model consists of the input layer, the output layer, and the hidden layer. Neural Fitting app is used to select data, create and train a network, and evaluate its performance using mean square error and regression analysis. A two-layer feed-forward network

with sigmoid hidden neurons and linear output neurons, and can fit the multi-dimensional mapping problems arbitrarily well, given consistent data and enough neurons in its hidden layer. The network will be trained with Levenberg-Marquardt backpropagation algorithm, in which case scaled conjugate gradient backpropagation will be used. Levenberg-Marquardt algoruthm typically requires more memory but less time. Training automatically stops when generalization stops improving, as indicated by an increase in the mean square error of the validation samples. Mean squared error is the average squared difference between outputs and targets. Lower values are better. Zero means no error.

The number of elements in the input layer is nine (number of C, H, N, O, Al, Cl, F elements, formation enthalpy, loading density) and the number of elements in the output layer is eight (A, B, R_1, R_2, ω, E_0, D_j, P_j).

All elements of a data set of numeric inputs and a set of numeric targets are normalized in the range of -1 to 1, within value range of the sigmoid function, and used as the data set of the neural network. After training of the neural network, the output data are reconverted back to the normalized range to obtain the desired value. The input vectors and target vectors will be randomly divided into three sets, the validation and test data sets are each set to 15% of the original data, 70% of original data will beused for training. Training data are presented to the network during training, and the network is adjusted according to its error. Validation data are used to measure network generalization, and to halt traing when generalization stops improving. Testing data have no effect on training and so provide an independent measure of network performance during and after training. And, deciding the number of hidden layers and the number of neurons in the hidden layers is a very important part of deciding your overall neural network architecture. Though hidden layers do not directly interact with the external environment, they have a tremendous influence on the final output. Both the number of hidden layers and the number of neurons in each of these hidden layers must be carefully considered. Using too few neurons in the hidden layers will result in something called underfitting. Underfitting occurs when there are too few neurons in the hidden layers to adequately detect the signals in a complicated data set. Using too many neurons in the hidden layers can result in several problems. First, too many neurons in the hidden layers may result in overfitting. Overfitting occurs when the neural network has so much information processing capacity that the limited amount of information contained in the training set is not enough to train all of the neurons in the hidden layers.

So, the network architecture should be changed, if the network training performance is poor. The specific number of neurons in the fitting network's hidden layers was determined by extensively iterative attempts. The rational network architecture is comprised one input layer, three hidden layers and one output layer, and number of neurons contained in each hidden layer was 237, 179 and 72 respectively. The following regression plots(Figure 1) display the network outputs with respect to targets for training, validation, and test sets.

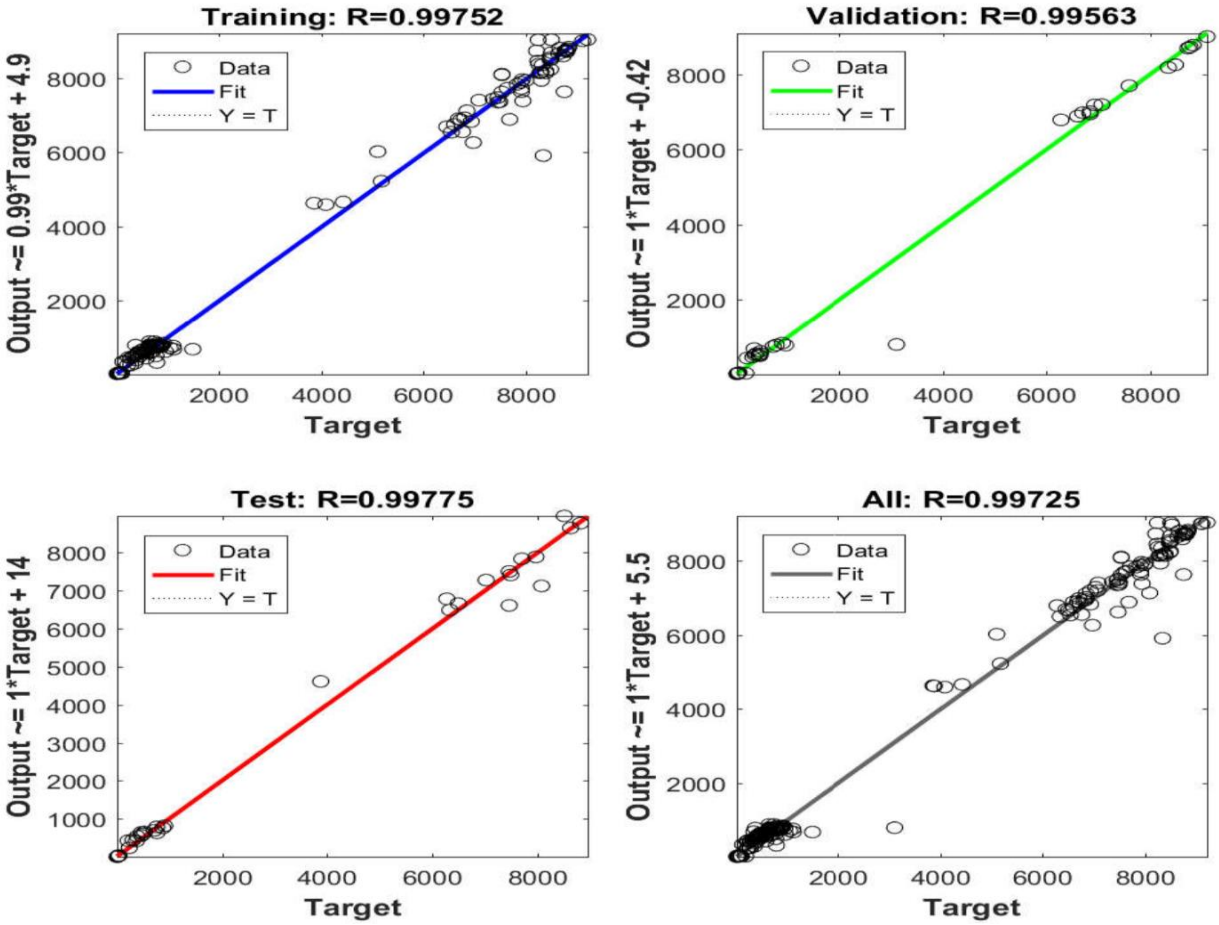

Fig. 1: *The network outputs with respect to targets for training, validation, and test sets*

No	Explosive Name	Number of elements per kg							ρ, g/cm³	Hf, kJ/kg	D_j, m/s	P_j, GPa	A, GPa	B, GPa	R_1	R_2	ω	E_0, GPa	Composition
		C	H	N	O	Al	Cl	F											
1	BTF	23.803	0	23.803	23.803	0	0	23.803	1.859	2386.86	8480	36	840.7	14.96	4.60	1.20	0.30	11.50	100 BTF
2	Comp A-3	18.675	37.822	24.585	24.585	0	0	18.675	1.65	134.61	8300	30	611.3	10.65	4.4	1.2	0.32	8.9	91RDX/9Wax
3	Comp B, Grade A	20.316	26.417	21.776	26.532	0	0	20.316	1.717	43.29	7980	29.5	524.2	7.678	4.20	1.1	0.34	8.5	36TNT/63RDX/1 Wax
4	Cyclotol	17.491	25.867	23.841	26.879	0	0	17.491	1.754	137.76	8250	32	603.4	9.924	4.30	1.1	0.35	9.2	23TNT/77RDX
5	DIPAM	26.422	13.211	17.615	26.422	0	0	26.422	1.55	-62.64	6700	18	425.4	8.007	4.7	1.3	0.39	6.2	100 DIPAM
6	Explosive D	24.38	24.38	16.254	28.444	0	0	24.38	1.42	-1583.38	6500	16	300.7	3.94	4.30	1.2	0.35	5.4	100 Ammonium picrate
7	FEFO	16.622	18.746	12.497	31.244	0	0	16.622	1.59	-2320.46	7500	25	382.4	6.635	4.1	1.2	0.38	8	100 FEFO
8	H-6	18.871	26.117	16.12	20.083	7.413	0	18.871	1.76	-39.04	7470	24	758.07	8.513	4.90	1.1	0.2	10.3	30TNT/45RDX/20Al /5Wax
9	HMX	13.508	27.017	27.017	27.017	0	0	13.508	1.891	253.35	9110	42	778.3	7.071	4.2	1	0.3	10.5	100 HMX
10	HNS	31.099	13.328	13.328	26.657	0	0	31.099	1	173.71	5100	7.5	162.7	10.82	5.40	1.8	0.25	4.1	100 HNS
11	HNS	31.099	13.328	13.328	26.657	0	0	31.099	1.4	173.71	6340	14.5	366.5	6.75	4.8	1.4	0.32	6	100 HNS
12	HNS	31.099	13.328	13.328	26.657	0	0	31.099	1.65	173.71	7030	21.5	463.1	8.873	4.55	1.35	0.35	7.45	100 HNS

No	Explosive Name	Number of elements per kg							ρ, g/cm³	Hf, kJ/kg	D_j, m/s	P_j, GPa	A, GPa	B, GPa	R_1	R_2	ω	E_0, GPa	Composition
		C	H	N	O	Al	Cl	F											
13	LX-01	15.25	37.279	16.942	33.884	0	0	15.25	1.23	-1182.16	6840	25.5	311	4.761	4.5	1	0.35	6.1	51.7NM/33.2TNM /15.1 1-Nitroproane
14	LX-04-1	15.491	25.77	22.964	22.964	0	0	15.491	1.865	-900.83	8470	34	836.4	12.98	4.62	1.25	0.42	9.5	85HMX/15Viton A
15	LX-07	14.83	26.186	24.315	24.315	0	0	14.83	1.865	-516.11	8640	35.5	871	13.9	4.6	1.15	0.3	10	90HMX/10Vition A
16	LX-09-1	14.256	27.362	25.925	27.218	0	0	14.256	1.84	83.84	8840	37.5	848.1	17.1	4.58	1.25	0.4	10.5	93.3HMX/4.4pDNPA /2.3FEFO
17	LX-10-1	14.235	26.56	25.531	25.531	0	0	14.235	1.865	-169.85	8820	37.5	880.7	18.36	4.62	1.32	0.38	10.4	94.5HMX/5.5Vition A
18	LX-11	16.152	25.355	21.613	21.613	0	0	16.152	1.875	-1285.26	8320	33	779.06	10.6678	4.5	1.15	0.3	9	80HMX/20Vition A
19	LX-14-0	15.211	29.172	25.886	25.592	0	0	15.211	1.835	63.49	8800	37	826.1	17.24	4.55	1.32	0.38	10.2	95.5HMX/4.5Estane5702-F1
20	NM	16.385	49.156	16.385	32.771	0	0	16.385	1.128	-1855.82	6280	12.5	209.2	5.689	4.40	1.2	0.3	5.1	100 Nitromethane
21	Octol	17.318	25.917	23.979	26.885	0	0	17.318	1.821	125.42	8480	34.2	748.6	13.38	4.5	1.2	0.38	9.6	22TNT/78HMX
22	PBX-9010	14.092	24.799	24.315	24.315	0	0.726	14.092	1.787	86.3	8390	34	581.4	6.801	4.10	1	0.35	9	90RDX/10Kel-F 3700
23	PBX-9011	17.292	31807	24.505	26.073	0	0	17.292	1.777	-168.56	8500	34	634.7	7.998	4.2	1	0.3	8.9	90HMX/10Estane 5703-F1
24	PBX-9407	14.125	26.68	25.396	25.396	0	0.714	14.125	1.6	33.4	7910	26.5	573.187	14.639	4.6	1.4	0.32	8.6	94RDX/6FPC 461

No	Explosive Name	Number of elements per kg							ρ, g/cm³	Hf, kJ/kg	D_j, m/s	P_j, GPa	A, GPa	B, GPa	R_1	R_2	ω	E_0, GPa	Composition
		C	H	N	O	Al	Cl	F											
25	PBX-9502	23.05	22.325	22.083	22.083	0	1.33	23.05	1.895	-858.95	7710	30.2	460.3	9.544	4	1.7	0.48	7.07	95TATB/5Kel-F 800
26	Pentolite	23.321	23.664	12.933	32.193	0	0	23.321	1.67	-894.36	7470	25	491.1	9.061	4.4	1.1	0.3	8	50TNT/50PETN
27	Pentolite	23.32	23.664	12.933	32.193	0	0	23.32	1.7	-894.36	7530	25.5	540.94	9.3726	4.50	1.1	0.35	8.1	50TNT/50PETN
28	PETN	15.819	25.311	12.655	37.966	0	0	15.819	0.88	-1460.61	5170	6.2	348.6	11.288	7	2	0.24	5.02	100 PETN
29	PETN	15.819	25.311	12.655	37.966	0	0	15.819	1.26	-1460.61	6540	14	573.1	20.16	6.00	1.8	0.28	7.19	100 PETN
30	PETN	15.819	25.311	12.655	37.966	0	0	15.819	1.5	-1460.61	7450	22	625.3	23.29	5.25	1.6	0.28	8.56	100 PETN
31	PETN	15.819	25.311	12.655	37.966	0	0	15.819	1.77	-1460.61	8300	33.5	617	16.926	4.40	1.2	0.25	10.1	100 PETN
32	Tetryl	24.381	17.514	17.415	27.865	0	0	24.381	1.73	110.76	7910	28.5	586.8	10.671	4.4	1.2	0.28	8.2	100 Tetryl
33	TNT	30.823	22.017	13.21	26.42	0	0	30.823	1.63	-328.12	6930	21	371.2	3.231	4.15	0.95	0.3	7	100 TNT
34	BTF	23.803	23.803	23.803	23.803	0	0	23.803	1.852	2386.86	8490	36	702.57	21.901	4.5	1.5	0.33	11.2	100 BTF
35	Comp-B	20.316	26.417	21.776	26.532	0	0	20.316	1.714	43.29	7900	31	488.96	28.264	4.5	1.5	0.3	9.4	63RDX/36TNT/1 Wax
36	FEFO	15.622	18.746	12.497	31.244	0	0	15.622	1.607	-2320.46	7450	24.1	464.96	12.455	4.5	1.5	0.31	9.3	100 FEFO
37	HMX	13.508	27.017	27.017	27.017	0	0	13.508	1.894	253.35	9100	40.8	881.453	20.902	4.5	1.5	0.34	11.4	100 HMX
3	HMX	13.50	27.01	27.01	27.01	0	0	13.50	1.18	253.35	6680	15.9	222.	12.6	4.5	1.5	0.3	7.2	100 HMX

No	Explosive Name	Number of elements per kg							ρ, g/cm³	Hf, kJ/kg	D_j, m/s	P_j, GPa	A, GPa	B, GPa	R_1	R_2	ω	E_0, GPa	Composition
		C	H	N	O	Al	Cl	F											
8		8	7	7	7			8	8				436	89					
39	HNS	31.099	13.328	13.328	26.657	0	0	31.099	1.681	173.71	7080	22.2	463.191	10.309	4.5	1.5	0.27	8.4	100 HNS
40	LX-04	15.491	25.77	22.964	22.964	0	0	15.491	1.869	-900.83	8490	35.5	744.45	20.923	4.5	1.5	0.33	9.3	85HMX/15Viton-A
41	Octol	17.837	25.767	23.565	26.867	0	0	17.837	1.809	107.98	8233	33.1	642.274	20.442	4.5	1.5	0.32	10.5	75HMX/25TNT
42	PBX-9404	14.011	27.537	25.653	26.899	0	0.315	14.011	1.842	23.6	8770	37.8	762.77	23.276	4.5	1.5	0.33	10.6	94HMX/3NC/3CEF
43	PBX-9404	14.011	27.537	25.653	26.899	0	0.315	14.011	1.844	23.6	8760	37.4	773.037	21.629	4.5	1.5	0.33	10.6	94HMX/3NC/3CEF
44	PETN	15.819	25.311	12.655	37.966	0	0	15.819	1.263	-1460.61	6760	16.6	264.744	11.501	4.5	1.5	0.25	8.1	100 PETN
45	PETN	15.819	25.311	12.655	37.966	0	0	15.819	1.503	-1460.61	7490	24	399.585	17.381	4.5	1.5	0.27	9.6	100 PETN
46	RX-27-AD	30.047	9.895	19.064	19.064	0	0.544	30.047	1.638	668.01	6930	20.6	437.298	9.548	4.5	1.5	0.3	7	92.5TACOT/7.5kel-F800
47	TNAZ	15.62	20.827	20.827	20.827	31.241	0	15.62	1.83	1359.5	8750	37.8	739.357	24.083	4.5	1.5	0.3	11.5	100 TNAZ
48	TNT	30.823	22.017	13.21	26.42	0	0	30.823	1.632	-328.12	7070	21.4	454.864	10.119	4.5	1.5	0.25	7.8	100 TNT
49	PETN	15.819	25.311	12.655	37.966	0	0	15.819	1.763	-1460.61	8274	31.5	1032.158	90.57	6	2.6	0.57	10.8	100 PETN
50	PETN	15.819	25.311	12.655	37.966	0	0	15.819	1.766	-1460.61	8283	33.1	622.045	21.465	4.5	1.5	0.29	11.2	100 PETN
5	LX-14	15.21	29.17	25.88	26.59	0	0	15.21	1.83	63.49	8830	38.1	755.	22.6	4.44	1.5	0.3	10.1	95.5HMX

No	Explosive Name	Number of elements per kg							ρ, g/cm³	Hf, kJ/kg	D_j, m/s	P_j, GPa	A, GPa	B, GPa	R_1	R_2	ω	E_0, GPa	Composition
		C	H	N	O	Al	Cl	F											
1		1	2	6	2			1	5				98	7					/4.5Estane5702-F1
52	LX-14	15.211	29.172	25.886	26.592	0	0	15.211	1.8358	63.49	8830	35.8	3104.4	174.43	7.66	2.65	0.4	9.5	95.5HMX /4.5Estane5702-F1
53	LX-14	15.211	29.172	25.886	26.592	0	0	15.211	1.825	63.49	8783	37.3	765.434	21.932	4.5	1.5	0.332	10.6	95.5HMX/4.5Estane5702-F1
54	LX-17	22.953	21.864	21.502	21.502	0	1.995	22.953	1.9	-944.28	7596	30	460.3	9.544	4	1.7	0.48	6.9	92.5TATB/7.5Kel-F 800
55	LX-17	22.953	21.864	21.502	21.502	0	1.995	22.953	1.909	-944.28	7636	27.4	692.131	7.15	4.5	1.5	0.26	8.6	92.5TATB/7.5Kel-F 800
56	AFX-902	10466	37.453	36.518	18.259	0	0	10466	1.742	-1147.06	8340	29.3	776.067	7.895	4.5	1.5	0.3	6.8	95NQ/5Viton-A
57	HNS	31.099	13.328	13.328	26.657	0	0	31.099	1.001	173.71	5100	7.7	112.502	4.767	4.5	1.5	0.31	4	100 HNS
58	NM	16.385	49.156	16.385	32.771	0	0	16.385	1.13	-1855.82	6280	13	198.182	8.723	4.5	1.5	0.34	5.69	100 Nitromethane
59	RX-26-AF	28.668	40851	17.849	22.789	0	0	28.668	1.844	-1341.96	8240	31.9	731.061	13.066	4.5	1.5	0.3	9.6	49.3HMX/46.6TATB /4.1estane
60	RX-39-AB	15.276	16.266	26.319	26.977	0	0	15.276	1.942	715.42	9208	43.3	908.741	24.627	4.5	1.5	0.34	11.8	95.8CL-20(epsilon) /4.2estane
61	TNM	5.102	0	20.409	40.818	0	0	5.102	1.65	188.12	6450	17.2	414.336	7.499	4.5	1.5	0.37	3.74	tetranitro-methane
62	TNT/Al	26.2	18.714	11.228	22.457	5.56	0	26.2	1.69	-278.9	6800	16.6	948	6.25	5.47	0.97	0.19	8.2	85TNT/15Al

No	Explosive Name	Number of elements per kg							ρ, g/cm³	Hf, kJ/kg	D_j, m/s	P_j, GPa	A, GPa	B, GPa	R_1	R_2	ω	E_0, GPa	Composition
		C	H	N	O	Al	Cl	F											
63	RDX/Wax	16.379	33.02	25.666	25.666	0	0	16.379	1.65	197.86	8390	28.4	1104.2	25.21	5.39	1.5	0.31	8.8	95RDX/5Wax
64	RDX	13.508	27.017	27.017	27.017	0	0	13.508	1.816	276.92	8661	32.6	634.7	8	4.2	1	0.3	5.0084	100 RDX
65	RDX/paraffin/graphite	16.620	30.145	25.666	25.666	0	0	16.620	1.667	197.23	8353	23.31	334.77	9.5009	6.71	1.26	0.21	9.396	95RDX/3parraffin /2graphite
66	RDX/Al/parraffin/graphite	15.269	27.443	22.964	22.964	3.706	0	15.269	1.72	169.54	8207	22.58	361.55	27.42	4.81	1.89	0.32	10.674	85RDX/10Al/3parraffin/2graphite
67	RDX/Al/parraffin/graphite	13.918	24.742	20.262	20.262	7.413	0	13.918	1.788	141.85	8087	22.04	709.6	20.274	5.37	1.9	0.34	12.438	75RDX/20Al/3parraffin/2graphite
68	RDX/Al/parraffin/graphite	12.567	22.040	17.561	17.561	11.119	0	12.567	1.853	114.16	7940	20.79	761.51	9.159	5.45	1.74	0.23	13.788	65RDX/30Al/3parraffin/2graphite
69	Lambrit	4.278	55.539	23.492	35.238	0	0	4.278	0.76	-4332.26	4084	3.455	203.582	2.973	6.651	1.127	0.39	2.049	94Amonium nitrate/6Disel Oil
70	Prillit A	4.278	55.539	23.492	35.238	0	0	4.278	0.85	-4332.26	3854	3.278	266.799	3.435	7.037	1.159	0.39	1.731	94Amonium nitrate/6Disel Oil
71	Nagolita	4.278	55.539	23.492	35.238	0	0	4.278	0.902	-4332.26	4426	4.503	207.791	2.914	5.907	1.079	0.4	2.293	94Amonium nitrate/6Disel Oil
72	A-U-100	4.278	55.539	23.492	35.238	0	0	4.278	0.83	-4332.26	3879	3.253	231.8	3.414	6.761	1.067	0.36	1.579	94Amonium nitrate/6Disel Oil
73	FH-5	16.379	33.020	25.666	25.666	0	0	16.379	1.6	197.86	7930	24.96	573.43	0.96006	4.275	0.3175	0.2178	8.7	95RDX/5wax
74	HMX/Wax	15.805	31.819	25.936	25.936	0	0	15.805	1.78	191.04	8730	33.5	1093.8	23.4	5.08	1.46	0.3	9.7	96HMX/4WAX
75	LX-07	14.830	26.186	24.315	24.315	0	0	14.830	1.865	-516.11	8640	35.5	871	13.896	4.6	1.15	0.3	10	90HMX/10VITON

No	Explosive Name	Number of elements per kg							ρ, g/cm³	Hf, kJ/kg	D_j, m/s	P_j, GPa	A, GPa	B, GPa	R_1	R_2	ω	E_0, GPa	Composition
		C	H	N	O	Al	Cl	F											
76	LX-11	16.152	25.355	21.613	21.613	0	0	16.152	1.875	-1285.56	8320	33	779.1	10.668	4.5	1.15	0.3	9	80HMX/20VITON
77	RX-04-DS	13.479	23.484	21.613	21.613	3.706	0	13.479	1.865	-541.44	8520	34	907.3	10.4	4.7	1	0.4	10.5	80HMX/10Al/10 VITON
78	X-0219	23.05	22.325	22.083	22.083	0	0.363	23.05	1.92	-1122.51	7530	26	626.8	8.48	4.8	1.2	0.35	6.8	90TATB/10Kel-F-800
79	HNS	31.099	13.328	13.328	26.657	0	0	31.099	1.54	173.71	6600	17.5	446.9	8.358	4.8	1.3	0.39	6	100 HNS
80	LX-17	22.953	21.864	21.502	21.502	0	0.544	22.953	1.905	-991.23	8000	27	1481.05	63.79	6.2	2.2	0.5	6.9	92.5TATB/7.5Kel F-800
81	TNT	30.823	22.017	13.21	26.42	0	0	30.823	1.5	-328.12	6603	17.784	303.588	3.1864	4.15	0.95	0.3	6.212	100 TNT
82	TNT	30.823	22.017	13.21	26.42	0	0	30.823	1.54	-328.12	6724	18.745	328.031	2.8877	4.15	0.95	0.3	6.45	100 TNT
83	TNT	30.823	22.017	13.21	26.42	0	0	30.823	1.58	-328.12	6843	19.897	350.32	3.093	4.15	0.95	0.3	6.69	100 TNT
84	TNT	30.823	22.017	13.21	26.42	0	0	30.823	1.61	-328.12	6845	21	371.2	3.23	4.15	0.95	0.3	7	100 TNT
85	PETN	15.819	25.311	12.655	37.966	0	0	15.819	1.75	-1460.61	7530	25.18	617	21.67	4.4	1.32	0.25	9.13	100 PETN
86	SEP	35.037	68.712	8.226	24.678	0	0	35.037	1.31	-1717.56	6970	15.91	364	2.31	4.3	1	0.28	2.82	65PETN/35Paraffin
87	RDX	13.508	27.017	27.017	27.017	0	0	13.508	1.777	276.92	8500	34	634.7	8	4.2	1	0.3	5.0084	100 RDX
88	HMX	13.508	27.017	27.017	27.017	0	0	13.508	1.783	253.35	8730	33.5	943.3	8.805	4.7	0.9	0.35	5.72	100 HMX
8	Pentolite	23.32	23.66	12.93	32.19	0	0	23.32	1.65	-894.36	7360	24.7	531.	8.93	4.6	1.05	0.33	8	50TNT/50PETN

No	Explosive Name	Number of elements per kg							ρ, g/cm^3	Hf, kJ/kg	D_j, m/s	P_j, GPa	A, GPa	B, GPa	R_1	R_2	ω	E_0, GPa	Composition
		C	H	N	O	Al	Cl	F											
9		1	4	3	3			1					77	3					
90	m/46	23.467	43.136	10.884	32.651	0	0	23.467	1.5	-1579.03	7680	21.15	759.9	12.56	5.1	1.5	0.29	7.05	86PETN/14% fuel oil
91	BTF/Al	19.836	0	19.836	19.836	6.177	0	19.836	1.762	1989.05	7829	26.9	698.69	6.1889	4.5796	0.92058	0.333	8.01	85BTF/15Al

For a perfect fit, the data should fall along a 45 degree line, where the network outputs are equal to the targets.

Regression R values measure the correlation between outputs and targets. An R value of 1 means a close relationship, 0 a random relationship. For this case, the fit is reasonably good for all data sets, with R values in each case of above 0.99.

3. Results and discussion

3.1. Prediction of JWL EOS parameters, detonation velocity and detonation pressure

For the new compositions of explosives not included in the training data set, the parameters of the JWL state equation, the detonation velocity and the detonation pressure were predicted.

The input data for the neural network are shown in Table 2. The neural network output data for each explosive are shown in Table 3.

Table 2: *Input data set*

No	Composition	ρ, g/cm^3	Hf, kJ/kg	Number of elements per kg					
				C	H	N	O	Al	Cl
1	95RDX/3WAX/ 2Stearic acid	1.5	156.65	16.22	32.609	25.666	25.806	0.0	0.0
		1.6	156.65	16.22	32.609	25.666	25.806	0.0	0.0
2	60TNT/24RDX/ 16Al	1.7	-130.41	21.736	19.694	14.410	22.336	5.930	0.0
		1.65	-130.41	21.736	19.694	14.410	22.336	5.930	0.0
3	50AP/25Al/ 25RDX	1.5	-1190.14	3.377	23.780	11.011	23.780	9.266	4.256
		1.6	-1190.14	3.377	23.780	11.011	23.780	9.266	4.256

Table 3: *Output data set*

No	Composition	ρ, g/cm^3	JWL EOS parameters and Detonation parameters							
			A, GPa	B, GPa	R_1	R_2	ω	E_0, GPa	D_j, m/s	P_j, GPa
1	95RDX/3WAX/ 2Stearic acid	1.5	653.785	10.679	5.00	0.91	0.24	8.97	7592.161	22.326
		1.6	802.163	11.142	5.00	0.84	0.24	9.63	7972.912	25.717
2	60TNT/24RDX /16Al	1.7	573.285	6.012	5.00	1.12	0.24	12.71	6740.002	19.638
		1.65	531.223	4.929	5.00	1.01	0.24	12.28	6589.502	18.273
3	50AP/25Al /25RDX	1.5	258.121	1.678	4.05	0.80	0.24	12.80	6631.984	19.121
		1.6	291.039	1.350	4.00	0.80	0.24	13.75	6841.922	21.559

3.2. Experimental validation

3.2.1. Comparison of detonation velocity prediction values with experimental values

Detonation velocity is defined as the velocity at which the chemical reaction zone propagates through a given explosive and is considered as one of the most important physical detonation parameters. The

determination of detonation velocity is based upon measurement of the time interval needed for the detonation wave to travel a known distance through the explosive under test. The method used to determine VOD is pin oscillographic technique (POT).

The Pin Oscillographic Technique is a discrete measurement technique using pin type ionization probes as sensors for detecting the arrival time of detonation wave at predetermined points and measuring propagation time between these points with the help of a high - speed oscilloscope.

The schematic of instrumentation set - up for VOD Determination by pin oscillographic technique is shown in Figure2.

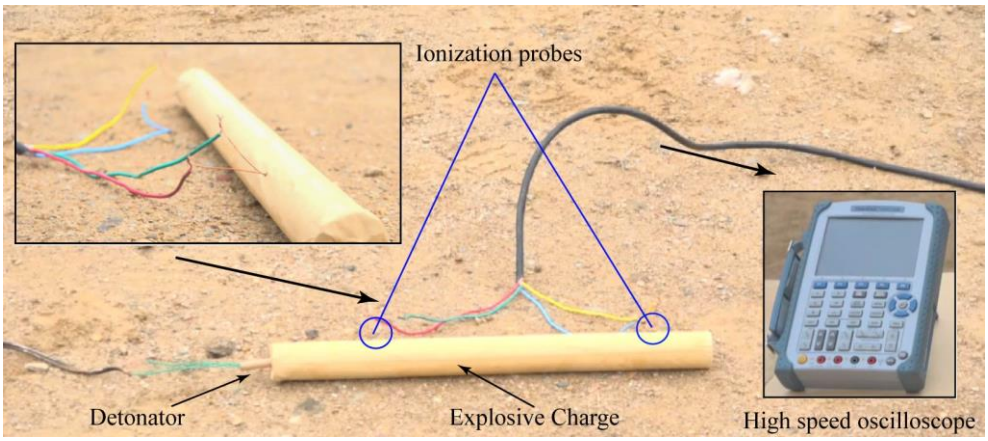

Fig. 2: *The schematic of instrumentation set – up for VOD Determination by pin oscillographic technique*

Digital storage oscilloscopes having 100/500MHz band width and sampling rate of 500 Mega sample per second (Ms s^{-1}) are being used to capture microsecond detonation events. This has a memory up to 50 Kbytes and the time base can be set from 2 nanosec/div.

Ionization probes get shorted due to the ionization of detonation products. The insulated copper wires of 0.8mm diameter and length 600 mm are taken and twisted together at the center followed by cutting of the twisted ends in the same plane.

The ionization probes are fixed at predetermined distances in the charge by inserting them 2~3 mm deep and securing with adhesive tape.

The distance of the first probe is generally 90 mm from the initiating end to allow the stabilization of the detonation wave. The second probe is fixed at a distance of 300 mm from first probe.

The charge is initiated by an electric detonator. The probes get shorted on arrival of the detonation wave and the pulses generated by the event box are stored on the high speed oscilloscope. The detonation velocity is then calculated as a quotient of the distance between two probes and corresponding time interval.

The relative error between the measured detonation velocity values and the predicted by the neural network is shown in Table 4. As relative error is less than 5%, it can be concluded that the predicted detonation velocity by neural network is relatively accurate.

Table 4: *The relative error for detonation velocity values*

No	Composition	Density, g/cm^3	Detonation velocity, m/s		Relative error, %
			Experimental	ANN	
1	95RDX/3WAX/2stearic acid	1.5	7304.6	7592.161	3.936711
		1.6	7804.3	7972.912	2.160501
2	60TNT/24RDX/16Al	1.7	6450.6	6740.002	4.486435
		1.65	6301.3	6589.502	4.573691
3	50AP/25Al/25RDX	1.5	6346.2	6631.984	4.50323
		1.6	6578.8	6841.922	3.999544

3.2.2 Comparition between experimental value and numerical simulation using the neural network output data

The accuracy of the JWL EOS parameters predicted by ANN is verified by the following method. When explosive charge with a given composition and density is detonated at a height of 1 m, the time-dependent blast shock wave overpressure is measured through a pressure sensors placed at a height of 1 m.

Then, explosive's explosion character is defined using the neural network output data, place the explosive charge and sensors exactly the same as the experiment, the time-dependent blast shock wave overpressure is obtained through numerical simulation. The generalization ability of neural network is evaluated by comparition between experimental values and numerical simulation results. Blast shock wave overpressure measurement test to be done as follows:

For each composition of explosive, 8 kg of explosive should be prepared.

Explosive charged into a cylindrical pipe with 20 cm in diameter and the explosive charge is placed at a height of 1 m from the ground. Pressure sensors are also installed at a height of 1 m from the ground and at 1 m intervals from 5 m away from the explosion center.

The explosion test was performed for the explosive charge 8 kg with different composition and density as shown in Fig. 3.

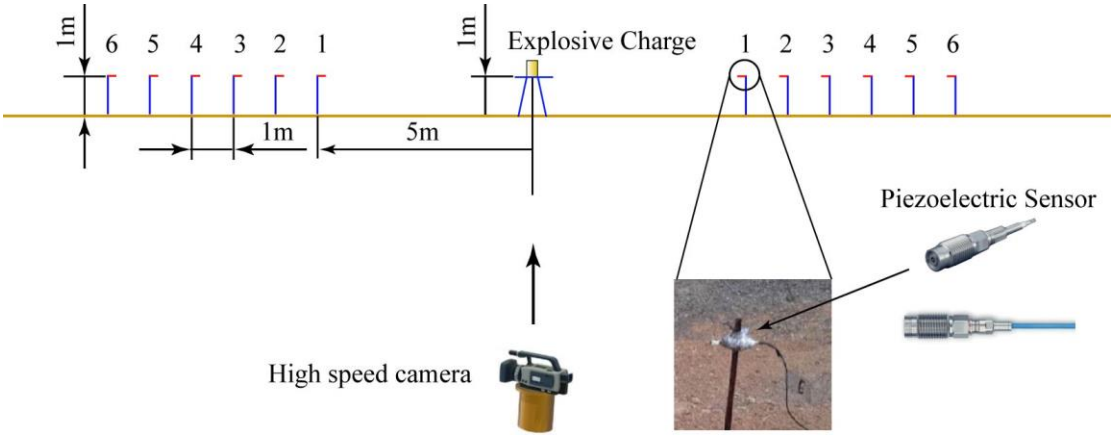

Fig 3: *Schematic of explosion shock wave overpressure measurement test*

The results of the blast shock-wave overpressure measurements at a height of 1 m from the ground at 5, 6, 7, 8, 9, and 10 m from the center of the explosion are presented in Table 5. As can be seen from Table 5, the blast shock wave overpressure at the measurement points is 0.1~0.25 kbar for three kinds of explosives.

Table 5: *Explosion shock wave overpressure*

No	Composition	Density, g/cm^3	Explosion shock wave overpressure according to position of sensors, kbar					
			1	2	3	4	5	6
1	95RDX/3WAX /2Stearic acid	1.5	0.227	0.207	0.189	0.175	0.168	0.156
		1.6	0.229	0.209	0.192	0.177	0.169	0.157
2	60TNT/24RDX/16Al	1.7	0.235	0.206	0.196	0.181	0.17	0.161
		1.65	0.233	0.199	0.193	0.179	0.169	0.16
3	50AP/25Al/25RDX	1.5	0.247	0.222	0.202	0.188	0.175	0.163
		1.6	0.246	0.221	0.202	0.187	0.176	0.165

Each explosion test has been shot using a high-speed camera, and Fig. 4 is shown the explosion process for 8 kg of 50AP/25Al/25RDX explosive charge with a density of 1.6 g/cm^3.

As shown in Fig. 4, the size of the explosion cloud is about 8 m in diameter, and the explosion products propagating along the ground can be observed. A region of 10 m height and 10 m radius was created, and then 2D simulations were performed using the solver used Euler and 2D Multi-materialization.

By defining the parameters of Table 3 in AUTODYN, a new explosive property was created, and the explosive charge and pressure measurement points were placed as shown in Fig. 3, and the results are shown in Fig. 5. The mesh size is determined by the following equation [17].

$$h_{iR} = n_{iR}\sqrt[3]{W}(mm) \quad (1)$$

Here, the recommended mesh size h_{iR} is defined as the product of the recommended scale coefficient n_{iR} and the third root of explosive mass $\sqrt[3]{W}$. The recommended scale coefficient n_{iR} is related to the scale distance, and the scale distance Z is 1m/kg$^{1/3}$.

For the convenience of application, the recommended scale coeffcient n_{iR} of 2D model is piecewise linear fitted with Z, as shown in Table 6.

Table 6: *The recommended scale coefficient n_{2R} of 2D model*

Z	0.06-0.07	0.07-0.08	0.08	0.08-0.09	0.09-6	0.6-0.8	0.8-1	1-1.5	1.5-2	2-3	≥3
n_{2R}	0.125	12.5Z-0.75	0.25	25Z-1.75	0.5	2.5Z-1	5Z-3	2	16Z-22	20Z-30	30

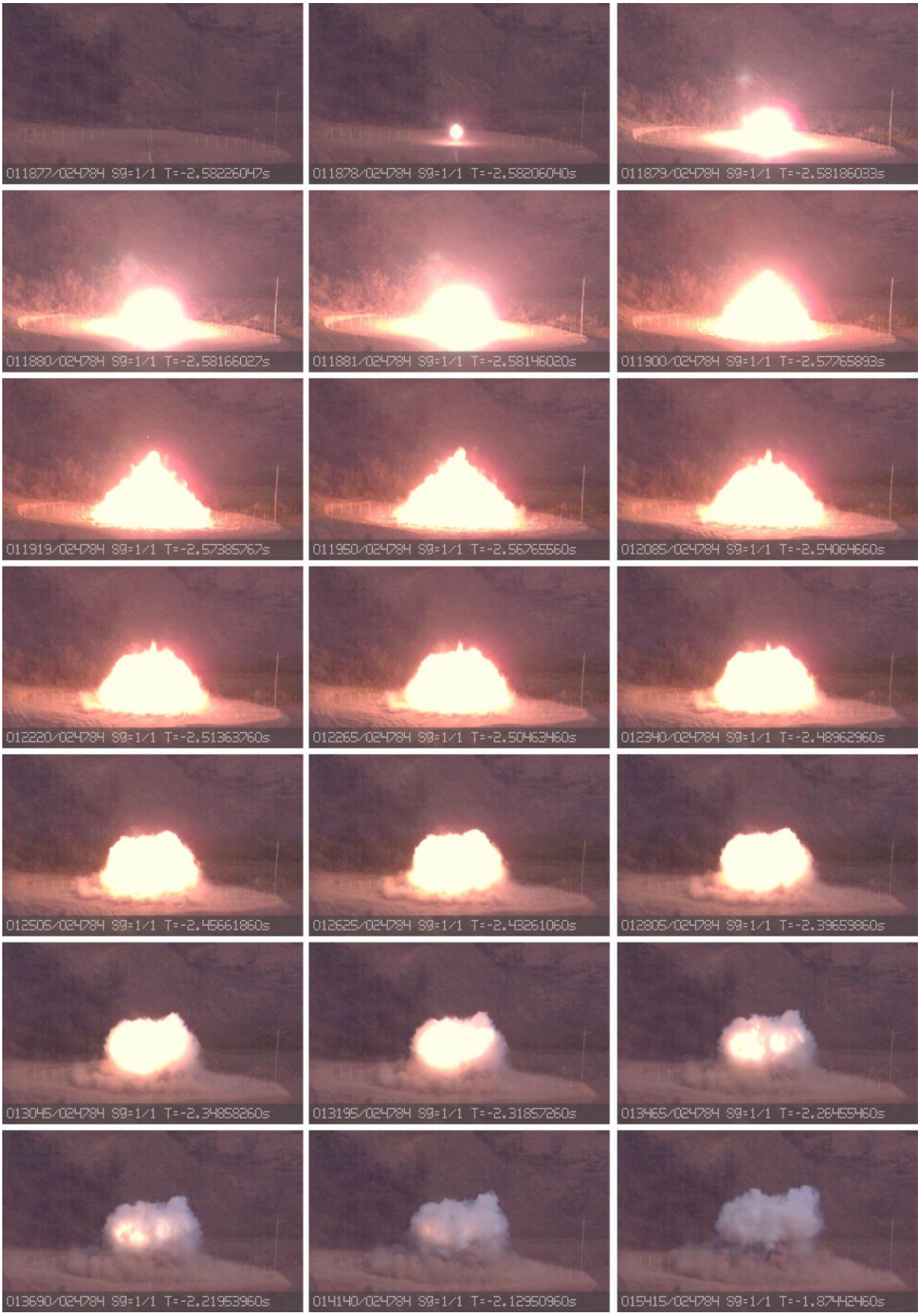

Fig. 4: *Explosion process of for 8 kg of 50 AP/25 Al/25 RDX explosive charge*

with a density of 1.6 g/cm^3

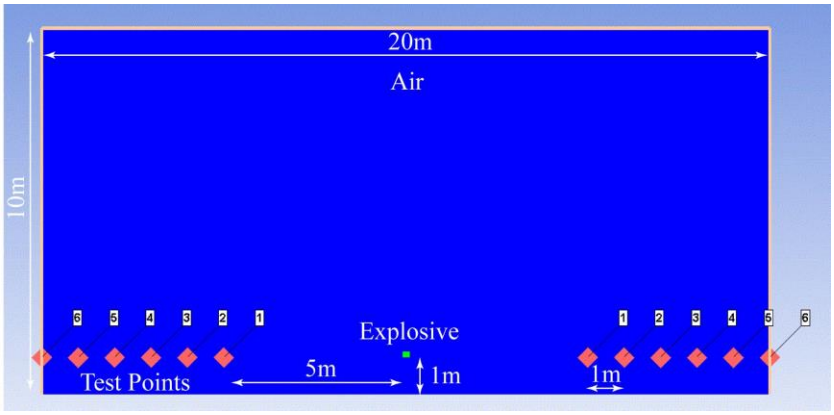

Fig. 5: *Schematic of explosion simulation in AUTODYN*

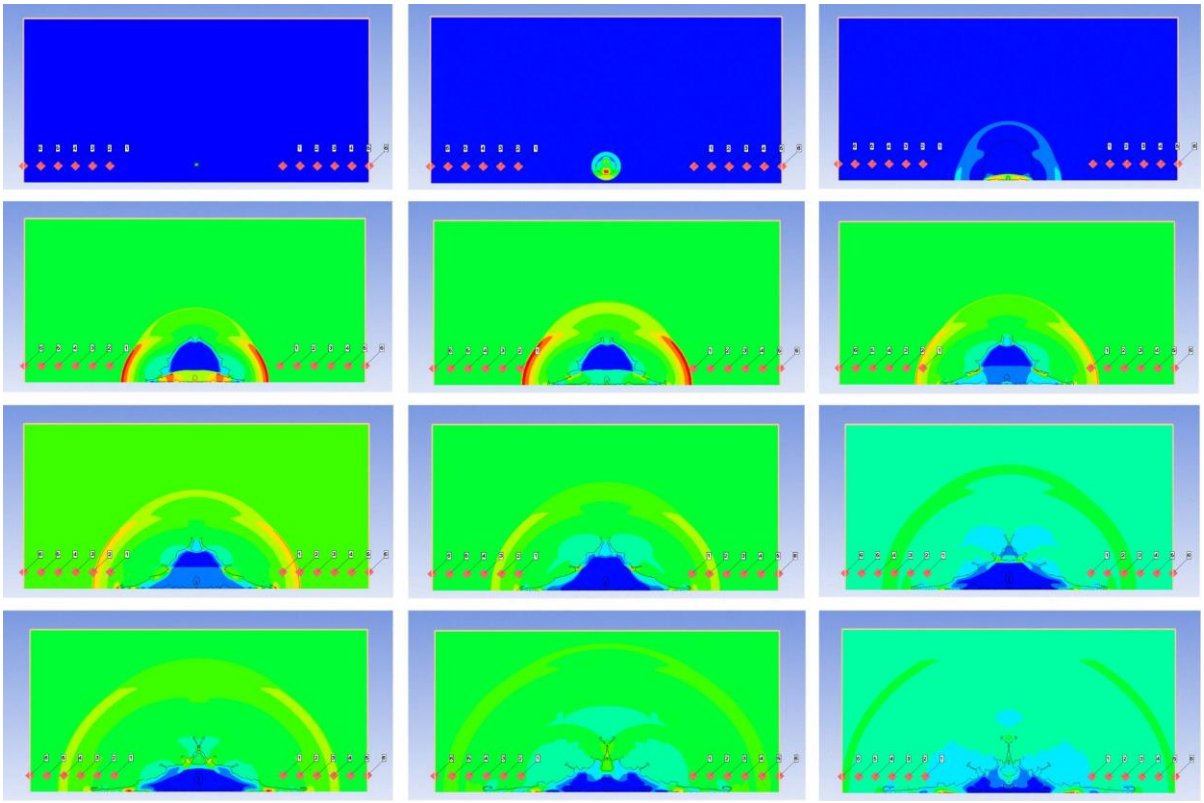

Fig. 6: *Explosion process of 8 kg of 50AP/25Al/25RDX explosive charge*

with a density of 1.6 g/cm^3

By substituting the recommended scale coeffcient n_{2R}(=30) given in Tables 8 into Eq. (1), the recommended mesh size of explosive charge of 8kg in 2D models at a specifc scaled distance(Z=5) can be obtained, the result is 60mm. Explosion simulations were carried out to analyze the phenomena occurring during explosions, and then investigate the time-dependent pressure variation at six measurement points.

The simulation result about explosion process of 8 kg of 50AP/25Al/25RDX explosive charge with a density of 1.6 g/cm^3 are shown in Fig. 6.

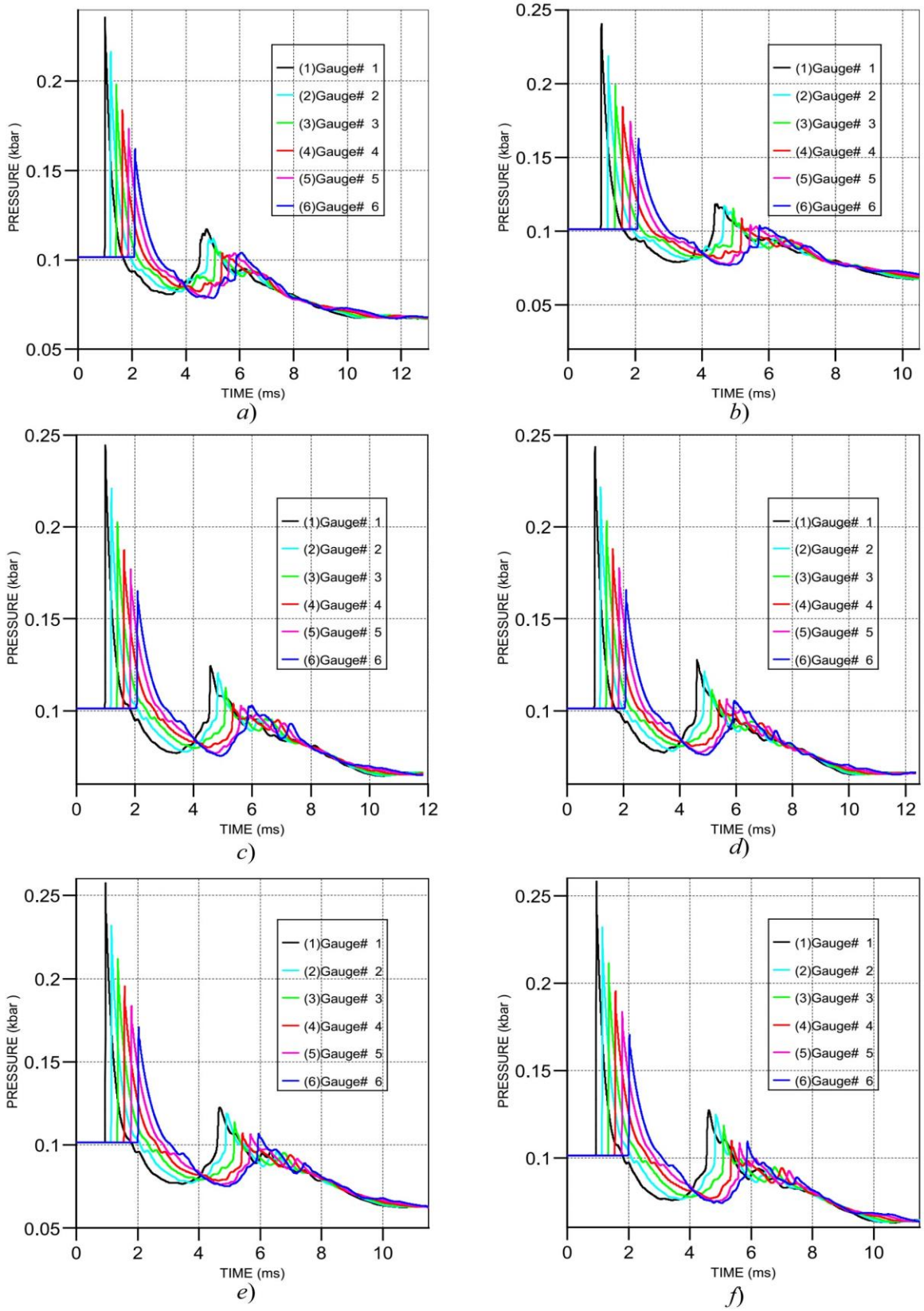

Fig. 7: *Time-dependent pressure variation characteristics at different measuring points.*

a-95RDX/3WAX/2stearic acid(1.5g/cm^3), b-95RDX/3WAX/2 stearic acid (1.6g/cm^3), c-60TNT/24RDX/16Al(1.7g/cm^3), d-60TNT/24RDX/16Al(1.65g/cm^3), e-50AP/25Al/25RDX(1.5g/cm^3), f-50AP/25Al/25RDX(1.6g/cm^3)

The shock wave formation process was analyzed in detail and it can be seen that the explosion product expansion process is very similar to the experimental data, shown Fig. 4.

The pressure profiles at the measurement points are shown in Fig. 7 and maximum of the shock wave overpressure at each measurement points are shown in Table 7.

The relative error between experimental data presented in Table 5 and the numerical simulation results presented in Table 7 was calculated at every measuring point and the results shown in Table 8. As shown in Table 8, the relative error between experimental results and numerical simulations results for the shock wave overpressure is less than 5%. It is found that the JWL EOS parameters determination method by neural network is valid.

Table 7: *Explosion shock wave overpressure*

No	Composition	Density, g/cm^3	Explosion shock wave overpressure according to position of sensors, kbar					
			1	2	3	4	5	6
1	95RDX/3WAX /2Stearic acid	1.5	0.23560	0.21636	0.19815	0.18368	0.17322	0.16193
		1.6	0.24023	0.21828	0.1986	0.18406	0.17415	0.16235
2	60TNT/24RDX /16Al	1.7	0.24434	0.2156	0.20300	0.18794	0.17735	0.16550
		1.65	0.24343	0.2087	0.20248	0.18720	0.17673	0.16495
3	50AP/25Al/ 25RDX	1.5	0.25732	0.23175	0.21131	0.19528	0.18330	0.17026
		1.6	0.25816	0.23179	0.21165	0.19537	0.18353	0.17063

Table 8: *Relative error of Explosion shock wave overpressure*

No	Composition	Density, g/cm^3	Relative error of Explosion shock wave overpressure according to position of sensors, %					
			1	2	3	4	5	6
1	95RDX/3WAX /2Stearic acid	1.5	3.78	4.52	4.84	4.96	3.10	3.80
		1.6	4.90	4.44	3.43	3.98	3.04	3.40
2	60TNT/24RDX /16Al	1.7	3.97	4.66	3.57	3.83	4.32	2.79
		1.65	4.47	4.87	4.91	4.58	4.57	3.09
3	50AP/25Al/ 25RDX	1.5	4.17	4.39	4.60	3.87	4.74	4.45
		1.6	4.94	4.88	4.77	4.47	4.27	3.41

4. CONCLUSIONS

The JWL EOS parameters and detonation parameters were collected according to composition of explosives, density and formation heat for 91 materials. Neural Network Fitting Tool of Matlab and Levenberg-Marquardt backpropagation algorithm was used for network training.

The rational neural network architecture consists of the input layer, output layer and hidden layer, and three hidden layers have 237, 179 and 72 neurons, respectively.

The fit is reasonably good for for training, validation, and test sets, with R values in each case of above 0.99. Based on Pin Oscillographic Technique, detonation velocity was measured for

three explosives (95RDX/3WAX/2stearic acid, 60TNT/24RDX/16Al, and 50AP/25Al/25RDX) with two densities, respectively.

The relative error for detonation velocity between ANN results and experimental results is less than 5%. To evaluate the generalization performance of the neural network, difference for the explosion shock overpressure between the experimental values and numerical simulation results were analyzed, the relative error is less than 5%.

It can be seen that the JWL EOS parameters prediction method by neural network are relatively accurate and can be useful for research of explosive characterization.

CRediT authorship contribution statement

***Ik Hyon Mun*:** Conceptualization, Investigation, Visualization, Writing-original draft, Writing - review & editing.

Jin Guk Pak: Conceptualization, Methodology, Investigation, Writing - original draft, Writing - review & editing, Visualization, Supervision, Project administration.

***Chol Min Kim*:** Investigation, Visualization, Writing - review & editing, Supervision.

***Jong Ju Kang*:** Conceptualization, Validation, Writing – review & editing.

***Chang Song Paek*:** Conceptualization, Validation, Writing - review & editing, Supervision.

***Jong Hyok Kim*:** Investigation, Visualization, Writing - review & editing.

Declaration of Competing Interest

The authors declare that they have no known competing financial interests or personal relationships that could have appeared to influence the work reported in this paper.

Acknowledgements

This research did not receive any specific grant from funding agencies in the public, commercial, or not-for-profit sectors.

5. REFERENCES

1. Wu X, Long X, He B, et al. VLW equation of state of detonation products. Sci China, Ser B: Chem 2009;52:605e8. https://doi.org/10.1007/s11426-009-0094-z.

2. Lee, E., Finger, M., Collins, W., “JWL Equation of State Coefficients for High Explosives”, Lawrence Livermore Laboratory, Rept-UCID-16189, (1973)

3. Lan, I-F., Huang, S. C., Chen, C. Y., Niu, Y. M. & Shiuan, J. H. An improved simple method of deducing JWL parameters from cylinder expansion test. Propellants, Explos., Pyrotech. 18, 18–24. 1993. https://doi.org/10.1002/prep.19930180104

4. Elek, P. M., Dzingalasevic, V. V., Jaramaz, S. S. & Mickovic, D. M. Determination of detonation products equation of state from CYLEX test: analytical model and numerical analysis. Term. Sci. 19 (1), 35–48. (2015). https://doi.org/10.2298/TSCI121029138E.

5. Esen S, Nyberg U, Arai H, Ouchterlony F. Determination of the energetic characteristics of commercial explosives using the cylinder expansion test technique. Sweden: Swedish Blasting Research Centre och Luleå Tekniska Universitet, Stockholm och Luleå; 2005

6. Sanchidrian, J. A., Castedo, R. & Lopez, L. M. Determination of the JWL constants for ANFO and emulsion explosives from CYLEX test data. Cent. Eur. J. Energ. Mater. 12 (2), 177–194 (2015).

7. R. Castedo, M. Natale, L.M. López, J.A. Sanchidrián, A.P. Santos, J. Navarro, P. Segarra, Estimation of Jones-Wilkins-Lee parameters of emulsion explosives using cylinder tests and their numerical validation, International Journal of Rock Mechanics and Mining Sciences 112 (2018) 290–301. https://doi.org/10.1016/j.ijrmms.2018.10.027

8. Cui, H. et al. Probe cylinder test method and calibration of JWL equation of state of detonation products for TNT explosive. Chin. J. Energetic Mater. (2023), 31 (7), 707–713. https://doi.org/10.11943/CJEM2023066

9. Pang, S., Chen, X., Xu, J., Guo, Z. & Cao, X. Research on equation of state parameters for high-energy solid propellants based on improved cylinder test and particle swarm optimization. Def. Technol. (2024), 47, 152–163. https://doi.org/10.1016/j.dt.2024.12.001.

10. Chandrasekaran N, Oommen C, Kumar VRS, et al. Prediction of detonation velocity and NO composition of high energy C-H-N-O explosives by means of artificial neural networks. Propellants, Explos Pyrotech 2019;44:579-87. https://doi.org/10.1002/prep.201800325.

11. Robitaille PO, Abou-Rachid H, Brisson J. Dielectric constant predictions for energetic materials using quantum calculations. Def Technol 2021;17:1988. https://doi.org/10.1016/j.dt.2020.09.022.-9412.
Hou F, Ma Y, Hu Z, et al. Machine learning enabled quickly predicting of detonation properties of N-containing molecules for discovering new energetic materials. Adv Theory Simul 2021;4:2100057. https://doi.org/10.1002/adts.202100057.

13. Elton DC, Boukouvalas Z, Butrico MS, et al. Applying machine learning techniques to predict the properties of energetic materials. Sci Rep 2018;8:9059. https://doi.org/10.1038/s41598-018-27344-x.

14. Dobratz BM, Laboratory LLN. LLNL explosives handbook: properties of chemical explosives and explosive Simulants. Lawrence Livermore National Laboratory, University of California; 1985

15. Souers PC, Haselman LC. Detonation equation of state at LLNL. 1993. https://doi.org/10.2172/10166640. 1994.

16. Koli S, Chellapandi P, Bhaskara RL, et al. Study on JWL equation of state for the numerical simulation of near-field and far-field effects in underwater explosion scenario. Eng Sci Technol Int J 2020;23:758-68. https://doi.org/10.1016/j.jestch.2020.01.007

17. Zhingping Kuang, Zhonghui Liu, Study on the mesh size determination method of blast wave numerical simulation with strong applicability, Heliyon 9 (2023) e13714. https://doi.org/10.1016/j.heliyon.2023.e13714